Engineering Conformational Flexibility in the Lactose Permease of *Escherichia coli*: Use of Glycine-Scanning Mutagenesis To Rescue Mutant Glu325→Asp[†]

Adam B.Weinglass,[‡] Irina N. Smirnova,[‡] and H. Ronald Kaback*

Howard Hughes Medical Institute, Departments of Physiology and of Microbiology & Molecular Genetics, Molecular Biology Institute, University of California, Los Angeles, Los Angeles, California 90095-1662

Received September 14, 2000

ABSTRACT: Lactose/H^+ symport by lactose permease of *Escherichia coli* involves interactions between four irreplaceable charged residues in transmembrane helices that play essential roles in H^+ translocation and coupling [Glu269 (helix VIII) with His322 (helix X) and Arg302 (helix IX) with Glu325 (helix X)], as well as Glu126 (helix IV) and Arg144 (helix V) which are obligatory for substrate binding. The conservative mutation Glu325→Asp causes a 10-fold reduction in the V_{max} for active lactose transport and markedly decreased lactose-induced H^+ influx with no effect on exchange or counterflow, neither of which involves H^+ symport. Thus, shortening the side chain may weaken the interaction of the carboxyl group at position 325 with the guanidino group of Arg302. Therefore, Gly-scanning mutagenesis of helices IX and X and the intervening loop was employed systematically with mutant Glu325→Asp in an effort to rescue function by introducing conformational flexibility between the two helices. Five Gly replacement mutants in the Glu325→Asp background are identified that exhibit significantly higher transport activity. Furthermore, mutant Val316→Gly/Glu325→Asp catalyzes active transport, efflux, and lactose-induced H^+ influx with kinetic properties approaching those of wild-type permease. It is proposed that introduction of conformational flexibility at the interface between helices IX and X improves juxtapositioning between Arg302 and Asp325 during turnover, thereby allowing more effective deprotonation of the permease on the inner surface of the membrane [Sahin-Tóth, M., Karlin, A., and Kaback, H. R. (2000) *Proc. Natl. Acad. Sci. U.S.A. 97,* 10729−10732.

The lactose permease (lac permease),[1] encoded by the *lacY* gene of *Escherichia coli* (*1*), catalyzes galactoside/H^+ symport and is an important model for transport proteins from Archaea to the mammalian central nervous system that transduce free energy stored in electrochemical ion gradients into solute concentration gradients (reviewed in *2*−*4*). The permease has been solubilized and purified in a completely active state (reviewed in *5*) and functions as a monomer (see *6*). All available evidence (reviewed in *7*−*9*) indicates that the molecule contains 12 transmembrane helices connected by hydrophilic loops with both the N and C termini on the cytoplasmic face of the membrane (Figure 1). In a functional mutant devoid of native Cys residues, each residue has been replaced with Cys (reviewed in *9*). Analysis of the mutant library has led to the following developments (*10*): (a) The great majority of the mutants are expressed normally in the membrane and exhibit significant activity, and only six side chains are clearly irreplaceable for active transport—Glu126 (helix IV) and Arg144 (helix V), which are indispensable for substrate binding, and Glu269 (helix VIII), Arg302 (helix IX), His322, and Glu325 (helix X), which are critical for coupling sugar and H^+ translocation. (b) Helix packing, tilts, and ligand-induced conformational changes have been determined by using site-directed biochemical and biophysical techniques. (c) Positions that are accessible to solvent have been revealed (see *11*−*13*). (d) Positions where the reactivity of the Cys replacement is increased or decreased by ligand binding have been identified (*11*−*16*). (e) The permease has been shown to be a highly flexible molecule. (f) A working model describing a mechanism for lactose/H^+ symport has been described (see *17*).

Site-directed studies utilizing excimer fluorescence, engineered divalent metal binding sites, spin-labeling, and/or thiol cross-linking provide a strong indication that the four irreplaceable residues involved in H^+ translocation and coupling—Glu269 (helix VIII), Arg302 (helix IX), His322, and Glu325 (helix X)—are within close proximity (*18*−*21*). Furthermore, since interaction between Glu269 and His322 appears to be essential for high-affinity ligand binding (*17, 22*), it is likely that in the ground state Glu269 is charge-paired with His322 and Arg302 is charge-paired with Glu325 (*17, 22*). In addition, charge pairing between Glu126 (helix IV) and Arg144 (helix V) plays an obligatory role in substrate binding (*23*−*26*).

Glu325 is probably involved directly in H^+ translocation. Extensive mutagenesis and functional characterization reveal that neutral replacements for Glu325 lead to mutants that are specifically defective in all translocation reactions that involve H^+ symport, but bind ligand and catalyze counterflow and equilibrium exchange as well or better than wild

[†] This work was supported in part by NIH Grant DK51131 to H.R.K.

* To whom correspondence should be addressed at HHMI/UCLA, 5-748 MacDonald Research Laboratories, Box 951662, Los Angeles, CA 90095-1662. Telephone: (310) 206-5053, Telefax: (310) 206-8623, E-mail: RonaldK@HHMI.UCLA.edu.

[‡] A.B.W. and I.N.S. contributed equally to this work.

[1] Abbreviations: lac permease, lactose permease; TDG, D-galactopyranosyl-1-thio-β,D-galactopyranoside; RSO, right-side-out; KP_i, potassium phosphate; NEM, *N*-ethylmaleimide.

10.1021/bi002171m CCC: $20.00
Published on Web 12/29/2000

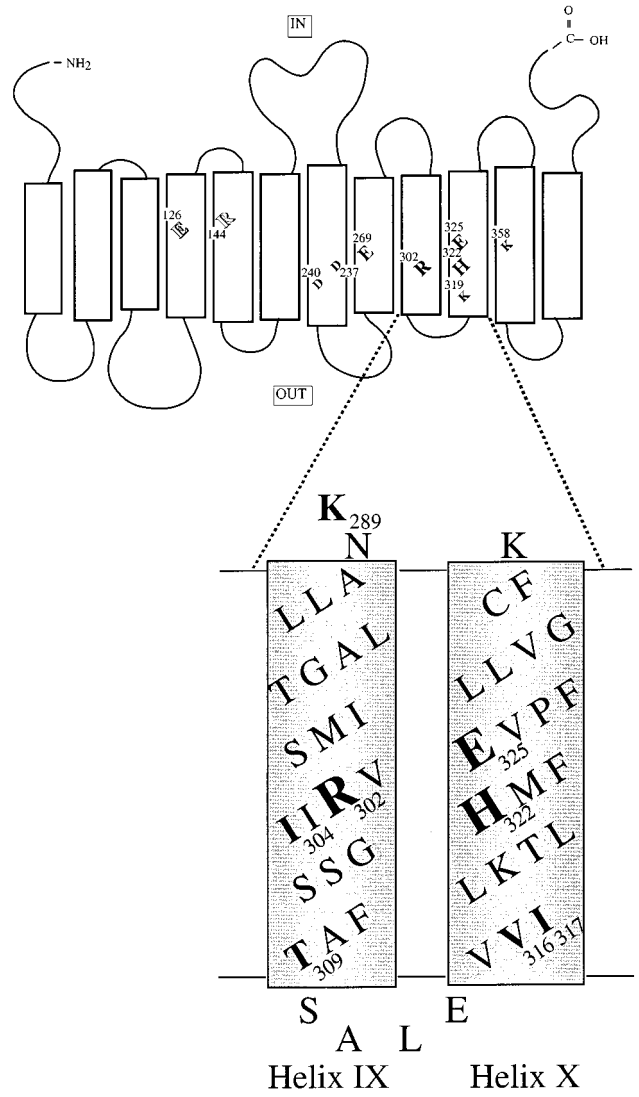

FIGURE 1: Seconday structure model of lac permease. Putative transmembrane helices are shown in boxes. Residues that are irreplaceable with respect to active transport are enlarged—Glu126 (helix IV) and Arg144 (helix V) are critical for substrate binding, and Glu269 (helix VIII), Arg302 (helix IX), His322 (helix X), and Glu325 (helix X) are essential for H^+ translocation and coupling. The charge pairs Asp237 (helix VII)/Lys358 (helix XI) and Asp240 (helix VII)/Lys319 (helix X) which do not play an essential role in the mechanism are also shown. Helices IX and X are amplified with Arg302, His322, and Glu325 enlarged and emboldened and positions where Gly replacement results in a significant increase in activity in mutant E325D emboldened.

type (*17, 27, 28*). Replacement of Glu325 with Asp yields permease that catalyzes active transport 15−20% as well as wild type and is markedly defective with respect to efflux down a concentration gradient (*28*). Furthermore, while mutant E325D[2] exhibits an increased K_D for ligand (i.e., lower affinity), neutral replacements for Glu325 have little or no effect on affinity (*17, 28*). Moreover, the apparent pK_a for ligand binding affinity by mutant E325Q is the same as that observed for the wild type or the E325D mutant, indicating that protonation of the carboxyl group at position 325 does not play a role in sugar binding (*17*).

[2] Site-directed mutants are designated as follows: the one-letter amino acid code is used followed by a number indicating the position of the residue which is followed by the desired mutation at the position.

When Glu126 (helix IV) is replaced with Asp, the permease exhibits relatively high activity (*25*), implying that helix V has sufficient flexibility to allow Arg144 to accommodate the decreased length of the carboxyl-containing side chain of Asp126. When conserved Gly residues lying one or two turns of an α-helix from Arg144 are replaced with Ala, there is little effect on the wild type; however, the mutations abolish substrate binding and transport in the E126D background. Furthermore, in two instances, significant activity is recovered when Ala residues at approximately parallel positions in helix IV are replaced with Gly. The findings suggest that the interface between helices IV and V is conformationally flexible (*29*).

In this communication, a similar approach is applied to mutant E325D. In an effort to compensate for the decrease in length of the carboxyl-containing side chain of the Asp residue in place of Glu325, 41 nonessential residues in helices IX and X were replaced systematically with Gly to increase conformational flexibility (Figure 1). Five mutants exhibit an increase in V_{max}, and mutant V316G/E325D catalyzes active transport, efflux, and lactose-induced H^+ influx with parameters approaching those of wild-type permease. Thus, introducing a Gly residue at the periplasmic end of helix X may improve interaction between Arg302 and Asp325, leading to more efficient deprotonation of the permease on the inner surface of the membrane after dissociation of sugar with rescue of lactose/H^+ symport activity.

EXPERIMENTAL PROCEDURES

Materials. Oligodeoxynucleotides were synthesized on an Applied Biosystems 391 DNA synthesizer. Restriction endonucleases, T4 DNA ligase, and Vent polymerase were from New England Biolabs (Beverly, MA), and Anti-His_5 antibody was purchased from Qiagen. All other materials were reagent grade and obtained from commercial sources.

Growth of Bacteria. *E. coli* T184 [*lacI*$^+$*O*$^+$*Z*$^-$*Y*$^-$*(A), rpsL, met*$^-$*, thr, recA, hsdM, hsdR/F′, lacI*^{q}*O*$^+$*Z*^{D118}*(Y*$^+$*A*$^+$*)*] (*30*) transformed with plasmid pT7-5/cassette *lacY* encoding given permease mutants was grown aerobically at 37 °C in Luria−Bertani broth with ampicillin (100 μg/mL). Fully grown cultures were diluted 10-fold and allowed to grow for 2 h at 37 °C before induction with 1 mM isopropyl 1-thio-β,D-galactopyranoside. After additional growth for 2 h at 37 °C, cells were harvested by centrifugation.

Construction of Permease Mutants. Using plasmid pT7-5/cassette *lacY* encoding mutant E325D permease, as indicated, oligonucleotide-directed site-specific mutagenesis by 2-step PCR (*31*) was used to replace each of 41 nonessential residues in helices IX and X and the intervening loop with Gly individually. Following restriction endonuclease digestion with *Kpn*I and *Spe*I, the PCR products were subcloned back into the similarly treated parental vector. The identical procedure was used to replace given residues in the same region with Gly in the wild-type background. Where indicated, following 2-step PCR to replace Cys333 with Ser, the *Kpn*I and *Spe*I restriction endonuclease fragments of E325D and V316G/E325D were cloned back into pT7-5/cassette *lacY* encoding single Cys148 permease with a C-terminal biotin acceptor domain (*32*). The *Kpn*I−*Spe*I region of the *lacY* gene in all mutants was fully sequenced through the restriction sites by using the dideoxynucleotide method (*33*) on an ABI 373A automatic sequencer.

Growth of Cells and Preparation of Right-Side-Out (RSO) Membrane Vesicles. E. coli T184 were grown in Luria−Bertani broth, and RSO membrane vesicles were prepared as described (*34*, *35*) except that 5.0 mM dithiothreitol (DTT) was included. At the end of the preparation, the vesicles were washed with 100 mM potassium phosphate (KP_i, pH 7.5) to remove DTT, resuspended in the same buffer at a protein concentration of 13−18 mg/mL, frozen in liquid N_2, and stored at −80 °C until use.

NEM Labeling. The reactivity of Cys148 with [^{14}C]NEM was determined in situ in the absence or presence of given concentrations of β-galactopyranosyl 1-thio-β-galactopyranoside (TDG) (*17*). Labeling at pH 7.5 was initiated by addition of 10 μL of [^{14}C]NEM to a final concentration of 0.5 mM (40 mCi/mmol), and the vesicles were incubated for 5 min at 25 °C as indicated. Reactions were quenched by addition of 10 mM DTT. Incorporation of [^{14}C]NEM was visualized and quantitated with a Storm 860 PhosphoImager. Apparent affinity constants (K_D^{app}) were determined with the MicroCalTMOrigin TM computer program using nonlinear least-squares curve fitting to a user-defined equation as described (*17*).

Transport Assays. E. coli T184 expressing given permease mutants were grown at 37 °C and subsequently washed once with 100 mM KP_i (pH 7.5)/10 mM $MgSO_4$ and adjusted to an optical density of 10.0 at 420 nm (0.7 mg of protein/mL). Transport was initiated by addition of [1-^{14}C]lactose (5 mCi/mmol) to a final concentration of 0.4 mM. Samples were quenched at given times with 100 mM KP_i (pH 5.5)/100 mM LiCl and assayed by rapid filtration (*36*). To determine kinetic parameters, cells were concentrated to an optical density of 20, and 50 μL of cells was mixed with 50 μL of [1-^{14}C]lactose (0.04−5 mM final concentrations). Initial rates were measured over 1 min for cells expressing wild-type permease and over 2 min for cells expressing E325D permease or derived mutants. Values were corrected for lactose uptake by cells carrying the pT7-5 vector with no *lacY* insert.

To measure lactose efflux, *E. coli* T184 cells expressing given permease mutants were resuspended at 3−4 mg of protein/mL in 100 mM KP_i (pH 7.5), ethylenediaminetetraacetate was added to a final concentration of 10 mM, and the suspensions were incubated at 37 °C for 2 min and placed on ice. Cells were then washed with 100 mM KP_i (pH 7.5) and resuspended in 100 mM KP_i (pH 7.5)/10 mM $MgSO_4$ before adjusting to an OD_{420} of 40.0 (2.8 mg of protein/mL). [1-^{14}C]Lactose (10 mM; 10 mCi/mmol) and 20 μM carbonyl cyanide *m*-chlorophenylhydrazone (CCCP) were added to each sample, and the suspensions were equilibriated on ice overnight. Aliquots (10 μL) of each sample were diluted 1:100 in KP_i (pH 7.5) containing 20 μM CCCP, and at given times, the reactions were quenched with 100 mM KP_i (pH 5.5)/100 mM LiCl and immediately filtered (*36*). Where indicated, preloaded cells were diluted 1:100 in 100 mM KP_i (pH 7.5)/20 μM CCCP and 10 mM NEM in addition to inactivate the permease. Zero time values were determined by dilution of 10 μL aliquots directly into quench buffer followed by rapid filtration.

Lactose-Induced H^+ Influx. Measurements were carried out essentially as described (*37*). Briefly, cells were washed twice in 1 mM KP_i (pH 7.5)/120 mM KCl and resuspended in 1 mM KP_i (pH 7.5)/120 mM KCl/30 mM KSCN to an OD_{420} of 80.0 (ca. 5.6 mg of protein/mL). An aliquot (0.5 mL) was placed in a closed, temperature-controlled glass cell under argon at 25 °C equipped with a glass pH electrode. Lactose was added to a final concentration of 15 mM in a 30 μL volume, and pH changes were recorded continuously. The signal was calibrated by addition of 5 μL of 10 mM HCl which corresponds to 50 nmol of H^+.

Western Blotting. Crude membranes from the same cells utilized for active transport assays were prepared by osmotic

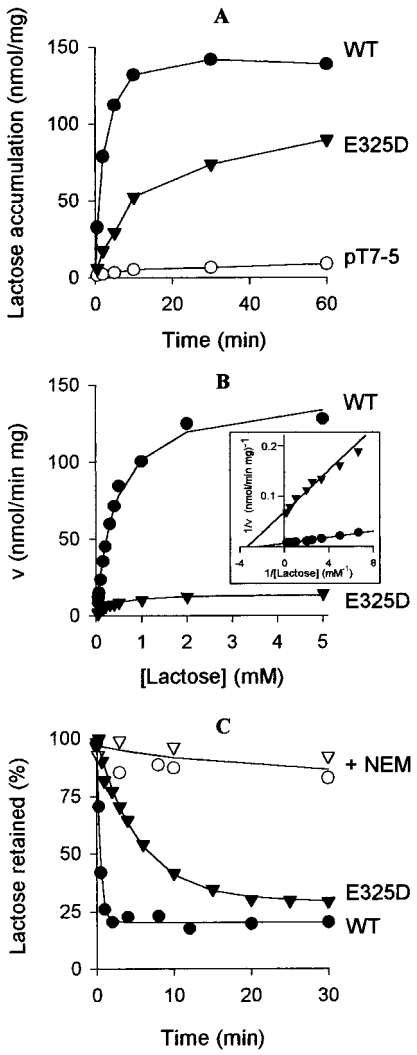

FIGURE 2: Wild-type permease versus mutant E325D. (A) Time courses of active transport by *E. coli* T184 expressing wild-type permease (WT), no permease (pT7-5 with no *lacY* insert), or the mutant E325D. Aliquots (50 μL) of cell suspensions containing 35 μg of protein in 100 mM KP_i (pH 7.5)/10 mM $MgSO_4$ were assayed at 0.4 mM final external concentration of lactose as described under Experimental Procedures. (B) Concentration-dependent lactose transport by *E. coli* T184 expressing wild-type permease or the mutant E325D. Initial rates of transport were determined at concentrations ranging from 40 μM to 5 mM [1-^{14}C]lactose as described under Experimental Procedures. For each data point, nonspecific lactose uptake by cells expressing no permease (pT7-5 with no *lacY* insert) was subtracted. Data were fitted to the Michaelis−Menten equation. Inset: double reciprocal plot. (C) Time course of lactose efflux by *E. coli* T184 expressing WT, no permease (pT7-5 only), or the mutant E325D. Aliquots of cells equilibrated with 10 mM [^{14}C]lactose in 100 mM KP_i (pH 7.5)/10 mM $MgSO_4$ and 20 μM CCCP were diluted 100-fold into the same solution without lactose as described under Experimental Procedures. Where indicated, NEM (10 mM, final concentration) was used to inactivate lac permease.

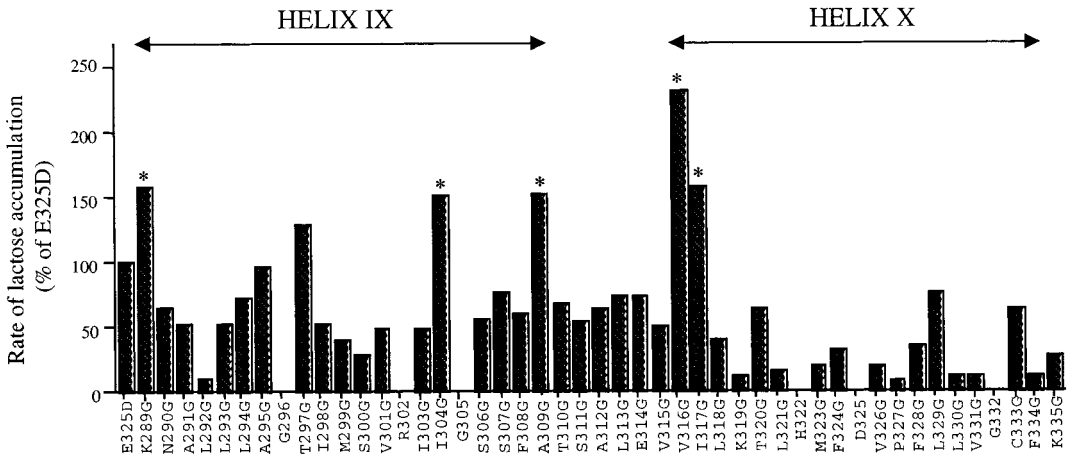

FIGURE 3: Active transport by *E. coli* T184 expressing E325D and individual Gly replacement mutants. The single-letter amino acid code is used along the horizontal axis to denote the original residues from Lys289 to Lys335. Mutants with significantly increased (>130%) activity are indicated with an asterisk (*). Rates of active transport were measured at 2 min as described under Experimental Procedures. Results are expressed as a percentage of E325D activity. Each bar in the histogram represents the average of at least 3 independent experiments, and the measurements did not vary by more than 20%.

lysis and sonication (*38*). Total membrane protein was assayed by a modified Lowry procedure (*39*). A sample containing 60 μg of membrane protein from each sample was subjected to electrophoresis in sodium dodecyl sulfate/12% polyacylamide gels (*40*). Proteins were electroblotted onto polyvinylidene fluoride membranes (Immobilon-PVDF; Millipore) and probed with site-directed antibody against the C-terminal 6-His tag on the permease followed by treatment with anti-mouse IgG-conjugated horseradish peroxidase.

RESULTS

Wild-Type Permease versus Mutant E325D. E. coli T184 (*lacZ*$^-$*Y*$^-$) expressing wild-type lac permease with 6-His residues at the C-terminus catalyzes lactose accumulation at a high rate to a steady-state level of ca. 150 nmol/mg of protein in approximately 10 min (Figure 2A). In contrast, as reported previously (*28, 41*), *E. coli* T184 expressing E325D permease catalyze accumulation at about 20% the rate of wild type, and by 1 h, the steady state is ca. 70% of wild type. Cells transformed with plasmid pT7-5 with no *lacY* insert exhibit negligible activity. Immunoblotting demonstrates that permease expression is comparable in cells expressing wild-type permease or the E325D mutant and undetectable in cells harboring plasmid pT7-5 with no *lacY* insert (data not shown; see *28*). Kinetic analysis reveals that while the K_m values for the wild type and the E325D mutant are similar [0.43 $\pm$ 0.03 and 0.3 $\pm$ 0.03 mM, respectively (Figure 2B)], the V_{max} observed for E325D is only 10% of wild type [15 $\pm$ 1 and 146 $\pm$ 4 μmol/(min·mg), respectively]. Furthermore, cells expressing wild-type permease catalyze lactose efflux down a concentration gradient ca. 20-fold more rapidly than cells expressing mutant E325D [$t_{1/2} \approx 0.17$ and 3.6 min, respectively (Figure 2C)]. Efflux from cells expressing either wild-type permease or mutant E325D after inactivation with NEM is extremely slow, reflecting non-permease-mediated passive diffusion.

Gly-Scanning Mutagenesis. In an effort to rescue activity in mutant E325D, each nonessential residue in helices IX and X and the intervening loop (see *9*) was replaced individually with Gly (Figure 3). Of the 41 mutants, 13 exhibit rates of lactose transport ranging from 0 to 30% of E325D, 23 exhibit rates ranging from 30 to 130% of E325D, and 5 exhibit rates of over 130% of E325D (Figure 3; *). To test whether the differences in activity observed are due to differences in permease expression, immunoblots were carried out on membrane preparations from the same cells on which transport was measured. With the exception of L292G, which is expressed poorly and exhibits very low activity, each of the other mutants is expressed in an amount comparable to E325D permease (data not shown).

Mutants with Highly Reduced Activity. Thirteen mutants display low rates of lactose transport (Figure 3). Eleven lie in helix X which contains the irreplaceable residues His322 and Glu325. Interestingly, with the exception of M323G which inactivates both the wild type and the E325D mutant, Gly replacements in close proximity to positions 322 or 325 are tolerated relatively well in the wild type, but lead to a marked loss of activity in the E325D background. Thus, mutants L321G (Figure 4A,B), F324G (Figure 4C,D), and V326G (Figure 4E,F), respectively, have relatively little effect on wild-type activity, while the same mutations cause significantly greater inhibition in the E325D background. The remaining mutants exhibit essentially the same low activities in both the wild-type and E325D backgrounds (F328G, L330G, V331G, F334G, and K335G). Neutral replacement of Lys319 (*42*−*44*) or Gly replacement for Pro327 (*45*) also inactivates the wild type, as shown previously, as well as the E325D mutant (not shown).

Mutant V316G. Five mutants in the E325D background (K289G, I304G, A309G, V316G, and I317G) exhibit significantly higher rates of transport than mutant E325D alone (Figure 3). To determine whether these effects are specific for the E325D mutant, the mutations were also characterized in the wild-type background. With the exception of mutant V316G which exhibits about 35% of the rate and 25% of the steady-state level of accumulation of wild-type permease at 0.4 mM lactose (Figure 5A), all of the other mutants in the wild-type background exhibit at least 75% of wild-type activity (data not shown). In contrast to the wild type, in the E325D background, all of these mutants exhibit significantly increased rates of transport, and in mutant V316G/E325D in particular, the rate is enhanced about 2.5-fold (Figure 5B).

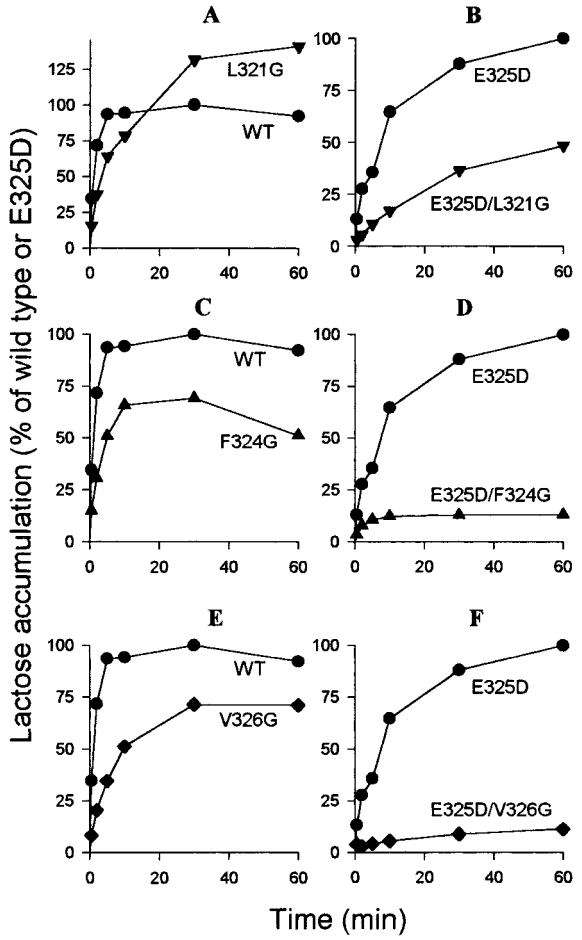

FIGURE 4: Effects of Gly replacement of residues near Glu325 or Asp325. Time courses of active transport by *E. coli* T184 expressing wild-type (WT) permease or E325D mutants with Gly in place of the native residue at positions 321 (A and B), 324 (C and D), or 326 (E and F). Experiments were carried out as described under Experimental Procedures. Data are plotted as percent maximum accumulation by wild type or E325D vs time.

Kinetic analysis of each mutant in the E325D background demonstrates that the K_m values of all five mutants with enhanced activity are generally similar to that of mutant E325D (Table 1). Furthermore, V316G/E325D exhibits a 3−4-fold increase in V_{max} (Table 1 and Figure 5D), while little or no effect is observed with V316G in the wild-type background (Figure 5C).

Replacement of Val316 with Gly also increases the rate of efflux about 3-fold in the E325D background [$t_{1/2} \approx 1.1$ min versus 3.8 min (Figures 5F)] and a minimum of 6-fold in the wild type [$t_{1/2} \approx 0.05$ min versus 0.3 min (Figure 5E)], which may account for the marked decrease in the steady-state level of accumulation.

Consistent with the 10-fold reduction in the V_{max} of lactose transport in cells with E325D, the rate of lactose-induced H^+ influx is much slower relative to cells with wild-type permease (Figure 6; see *41* in addition). Moreover, cells with wild-type permease containing the V316G mutation exhibit at least a 3-fold increase in H^+ influx, suggesting that the mutation results in partial uncoupling of lactose and H^+ translocation (Figure 6, insets). In contrast, a much more dramatic increase in lactose-induced H^+ influx is observed in cells expressing mutant V316G/E325D relative to E325D alone.

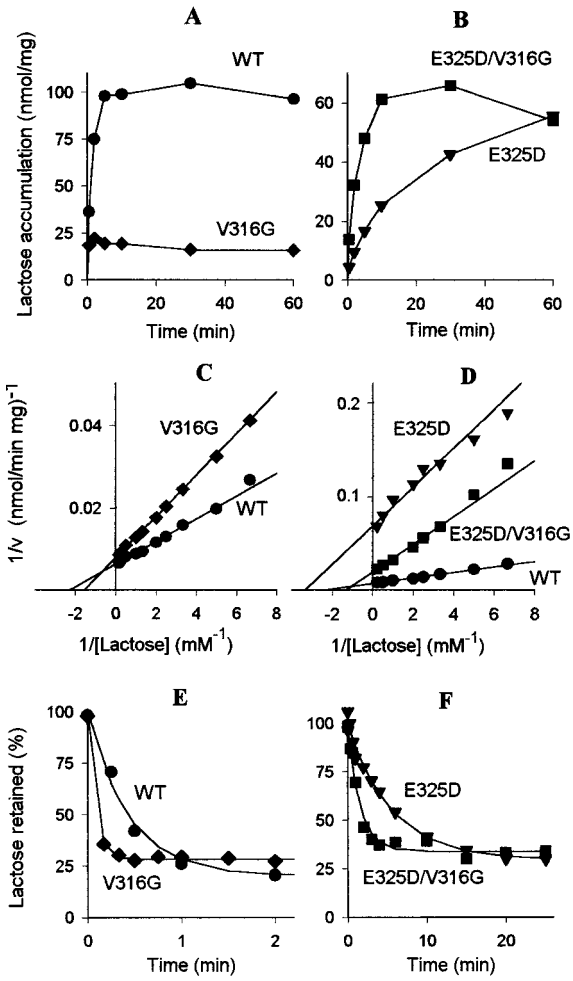

FIGURE 5: Transport properties of V316G or V316G/E325D permease. (A, B) Time courses of active transport. *E. coli* T184 expressing wild type (WT) or V316G (A) or E325D or V316G/E325D permease (B) were assayed as described in Figure 2A and under Experimental Procedures. (C, D) Kinetic analysis of active transport. Initial rates of transport by *E. coli* T184 expressing WT or V316G (C) or WT, E325D, or V316G/E325D permease (D) were determined at given lactose concentrations as described in Figure 2B and under Experimental Procedures. (E, F) Time courses of lactose efflux. *E. coli* T184 expressing WT or V316G (E) or E325D or V316G/E325D permease (F) were prepared and assayed as described in Figure 2C and under Experimental Procedures.

Table 1: Kinetic Properties of E325D Activating Gly Mutants[a]

mutant	V_{max} [nmol/(min·mg)]	K_m (mM)
WT	146 ± 4	0.43 ± 0.03
E325D	15 ± 1	0.30 ± 0.03
K289G/E325D	18 ± 1	0.40 ± 0.03
I304G/E325D	29 ± 1	0.57 ± 0.03
A309G/E325D	21 ± 1	0.40 ± 0.03
V316G/E325D	52 ± 1	0.76 ± 0.04
I317G/E325D	23 ± 1	0.38 ± 0.02

[a] Experiments were carried out as described under Experimental Procedures.

Since mutant E325D exhibits about a 10-fold decrease in affinity relative to the wild type or to neutral replacements for Glu325 (*17*, *28*), the increased activity of mutant V316G may be due to an increase in affinity for substrate. Therefore, the effect of the V316G mutation on the affinity of mutant E325D for β,D-galactopyranosyl 1-thio-β,D-galactopyranoside (TDG) was measured by introducing E325D or V316G/

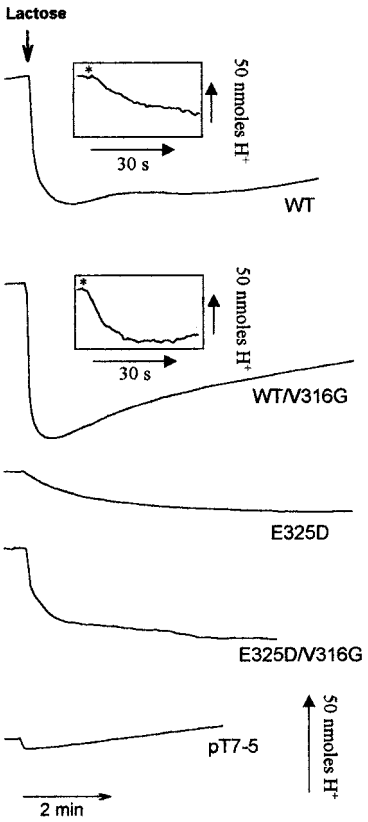

FIGURE 6: Lactose-induced H^+ uptake. *E. coli* T184 expressing wild type (WT), V316G, E325D, or V316G/E325D permease or no permease (pT7-5 with no *lacY* insert) were prepared as described under Experimental Procedures. Changes in the external pH upon addition of 15 mM lactose (final concentration) were monitored with a pH electrode as described under Experimental Procedures. Downward displacement indicates alkalinization of the external medium. Insets represent the same procedure time-resolved for 45 s after addition of 15 mM lactose (*).

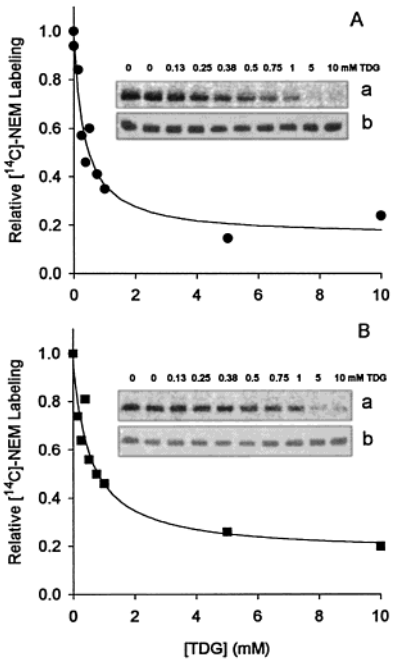

FIGURE 7: Substrate protection against alkylation of Cys148 by TDG. RSO membrane vesicles with either E325D (A) or V316G/E325D permease (B) with a single Cys residue at position 148 and a biotin-acceptor domain at the C-terminus were incubated in 100 mM KP_i (pH 7.5) with 0.5 mM [^{14}C]NEM at 25 °C for 5 min in the absence or the presence of indicated concentrations of TDG as described under Experimental Procedures. Reactions were quenched with DTT, and biotinylated permease was solubilized and purified by affinity chromatography on monomeric avidin. Aliquots of protein were separated on a 12% polyacrylamide gel, and ^{14}C-labeled protein was visualized by autoradiography (inset, a). A fraction of the protein was analyzed by Western blotting to determine the amount of permease in each sample (inset, b). Incorporation of [^{14}C]NEM was quantitated by a Storm 860 PhosphoImager, and the labeling in the presence of given concentrations of TDG is expressed as percent labeling observed in the absence of sugar.

E325D into permease with a single Cys residue at position148 and monitoring protection against alkylation by NEM as a function of TDG concentration (see *17*, *25*, *46*). Consistent with previous observations (*17*), mutant E325D exhibits a K_D^{app} of 350 ± 0.05 μM (Figure 7A), while V316G/E325D has a slightly elevated K_D^{app} of 580 ± 0.23 μM (Figure 7B).

DISCUSSION

Recent studies (*17*) in which ligand binding affinity was measured as a function of pH in single-Cys148 permease with various replacements for Glu269, Arg302, His322, and Glu325 have led to a working model describing a mechanism for lactose/H^+ symport. In the ground state, the permease is protonated, the H^+ is shared between His322 and Glu269, Glu325 is charge-paired with Arg302, and substrate is bound with high affinity between helices IV (Glu126) and V (Arg144 and Cys148) from the outside surface of the membrane. Substrate binding induces a conformational change that leads to transfer of the H^+ from His322/Glu269 to Glu325 and reorientation of the binding site to the inner surface with a decrease in affinity and dissociation of substrate. Glu325 is then deprotonated on the inside due to re-juxtapositioning with Arg302. The His322/Glu269 complex is then protonated from the outside to reinitiate the cycle.

Not surprisingly, the only replacement for Glu325 that catalyzes lactose/H^+ symport to any extent whatsoever is Asp. However, there is a 10-fold reduction in the V_{max} for active transport, as well as the rate and extent of lactose-induced H^+ influx under de-energized conditions. Furthermore, efflux down a lactose concentration gradient which also occurs in symport with H^+ (*47*) is also about 20-fold slower in cells with E325D than wild type. Consistent with the proposed mechanism, the distance between the shortened carboxyl side chain at position 325 and the guanidino group of Arg302 may be increased in E325D, thereby weakening the interaction between the carboxyl and guanidino side chains (*48*). Therefore, during lactose/H^+ symport, re-juxtapositioning between Arg302 and Asp325 may be less favorable, leading to reduction in the rate of deprotonation of Asp325 relative to Glu325 after dissociation of sugar on the inside of the membrane. Suggestive evidence for this notion is provided by comparison of mutants with Gly in place of residues in the vicinity of position 325 in the wild type or mutant E325D. While there is little significant effect on activity in the wild type, identical replacements in mutant E325D produce a marked reduction in activity (Figure 4). Thus, the distance between the carboxyl group at position 325 in helix X and the guanidino group at position 302 may

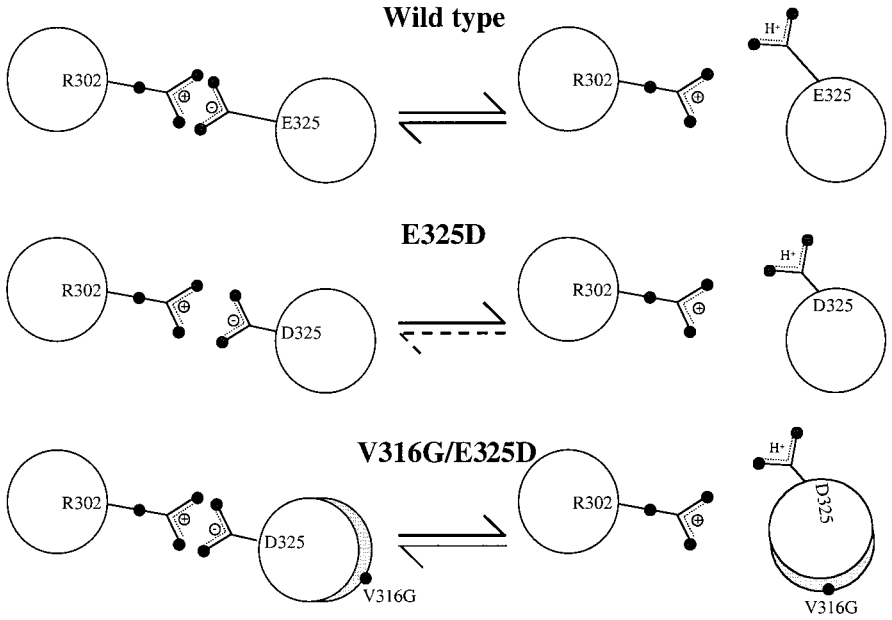

FIGURE 8: Introduction of conformational flexibility at position 316 re-juxtapositions Asp325 with Arg302, leading to enhanced deprotonation. An end-on view of helices IX and X with positions 302 and 325 is depicted. In wild type, E325D, or V316G/E325D permease, binding of lactose induces a conformational change leading to the transfer of the H^+ shared by His322/Glu269 to position 325, disrupting the charge pair with Arg302 (solid forward arrow) (*17*). Subsequently, following reorientation of the binding site to the inner surface with a decrease in affinity and dissociation of substrate in wild-type permease, Glu325 is deprotonated due to re-juxtapositioning with Arg302 (thick solid reverse arrow). In mutant E325D, shortening of the carboxylate side chain weakens interaction with Arg302, leading to less effective deprotonation (dashed reverse arrow). Introduction of conformational flexibility at position 316 permits rigid body movement of helix X, thereby allowing more effective re-juxtapositioning between Arg302 and Asp325 and more efficient deprotonation (thin solid reverse arrow).

be highly dependent upon structural perturbations in the immediate vicinity.

Each nonessential residue in helices IX and X and the intervening loop of E325D was replaced with Gly and screened for active transport in an effort to rescue activity by introducing conformational flexibility which might compensate for the shortened carboxyl-containing side chain of E325D. Five mutants with significantly greater activity than mutant E325D were identified, and four of the mutants are located at the putative boundaries of helices IX (K289G and A309G) and X (V316G and I317G), while one lies toward the center of helix IX (T304G). It is noteworthy that: (a) replacement of these native residues with Cys in Cys-less permease does not lead to increased activity (*38*); and (b) with the exception of V316G, the mutations have little or no effect on the wild-type. Furthermore, combining the three mutations clustered at the periplasmic ends of helices IX (A309G) and X (V316G and I317G) in mutant E325D does not lead to enhanced activity (data not shown).

Remarkably, all of the mutants with enhanced activity manifest increases in V_{max} with little if any change in K_m (Table 1). Furthermore, while mutant V316G/E325D, the most active, shows a slight increase in the apparent K_D^{app} for TDG binding relative to E325D, it exhibits a 4-fold increase in V_{max} paralleled by an increase in the rate of lactose-induced H^+ influx. Lactose efflux, a translocation reaction that also involves H^+ symport (*47*), is similarly enhanced in V316G/E325D, and at least a 6-fold increase in lactose efflux is observed with mutant V316G in the wild-type background as well. Furthermore, the V316G mutation in the wild-type background causes about a 3-fold increase in lactose-induced H^+ influx. Thus, taken together, the findings with mutant V316G in the wild-type versus the E325D backgrounds indicate that the mutation partially uncouples wild type and increases coupling in E325D permease. Although this may seem paradoxical, if efficient deprotonation of a carboxylic acid at position 325 (helix X) is dependent upon the frequency with which it re-juxtapositions with Arg302 (helix IX) after dissociation of sugar, such a possibility is not farfetched (Figure 8). With Glu at position 325, conditions are optimal for deprotonation, and introduction of conformational flexibility in the vicinity might cause significantly higher rates of deprotonation, leading to partial uncoupling of lactose and H^+ translocation which is reflected by a decreased steady-state level of accumulation, increased lactose-induced H^+ influx, and increased rates of efflux. In contrast, with the shortened side chain of Asp325, the distance between the carboxyl group and the guanidinium side chain of Arg302 would be greater, the frequency of re-juxtapositioning between the two side chains would be decreased, and the permease would be uncoupled. By increasing conformational flexibility with the introduction of the V316G mutation into mutant E325D, the frequency of re-juxtapositoning between the two side chains might be increased, thereby increasing the efficiency of lactose/H^+ symport with little or no change in affinity for substrate.

ACKNOWLEDGMENT

We thank Miklós Sahin-Tóth for helpful discussions and for critically reading the manuscipt, as well as Kerstin Stempel for synthesizing oligonucleotides.

REFERENCES

1. Müller-Hill, B. (1996) *The lac Operon: A Short History of a Genetic Paradigm*, Walter de Gruyter, Berlin and New York.
2. Kaback, H. R. (1976) *J. Cell. Physiol. 89*, 575−593.
3. Kaback, H. R. (1983) *J. Membr. Biol. 76*, 95−112.
4. Kaback, H. R. (1989) *Harvey Lect. 83*, 77−103.

5. Viitanen, P., Newman, M. J., Foster, D. L., Wilson, T. H., and Kaback, H. R. (1986) *Methods Enzymol. 125*, 429−452.
6. Sahin-Tóth, M., Lawrence, M. C., and Kaback, H. R. (1994) *Proc. Natl. Acad. Sci. U.S.A. 91*, 5421−5425.
7. Kaback, H. R. (1996) in *Handbook of Biological Physics: Transport Processes in Eukaryotic and Prokaryotic Organisms* (Konings, W. N., Kaback, H. R., and Lolkema, J. S., Eds.) pp 203−227, Elsevier, Amsterdam.
8. Kaback, H. R., and Wu, J. (1997) *Q. Rev. Biophys. 30*, 333−364.
9. Frillingos, S., Sahin-Tóth, M., Wu, J., and Kaback, H. R. (1998) *FASEB J. 12*, 1281−1299.
10. Kaback, H. R., and Wu, J. (1999) *Acc. Chem. Res. 32*, 805−813.
11. Venkatesan, P., Liu, Z., Hu, Y., and Kaback, H. R. (2000) *Biochemistry 39*, 10649−10655.
12. Venkatesan, P., Kwaw, I., Hu, Y., and Kaback, H. R. (2000) *Biochemistry 39*, 10641−10648.
13. Venkatesan, P., Yu, Y., and Kaback, H. R. (2000) *Biochemistry 39*, 10656−10661.
14. Frillingos, S., and Kaback, H. R. (1996) *Biochemistry 35*, 3950−3956.
15. Frillingos, S., Wu, J., Venkatesan, P., and Kaback, H. R. (1997) *Biochemistry 36*, 6408−6414.
16. Frillingos, S., and Kaback, H. R. (1997) *Protein Sci. 6*, 438−443.
17. Sahin-Tóth, M., Karlin, A., and Kaback, H. R. (2000) *Proc. Natl. Acad. Sci. U.S.A. 97*, 10729−10732.
18. Jung, K., Jung, H., Wu, J., Privé, G. G., and Kaback, H. R. (1993) *Biochemistry 32*, 12273−12278.
19. Jung, K., Voss, J., He, M., Hubbell, W. L., and Kaback, H. R. (1995) *Biochemistry 34*, 6272−6277.
20. He, M. M., Voss, J., Hubbell, W. L., and Kaback, H. R. (1995) *Biochemistry 34*, 15667−15670.
21. He, M., Voss, J., Hubbell, W. L., and Kaback, H. R. (1997) *Biochemistry 36*, 13682−13687.
22. He, M., and Kaback, H. R. (1997) *Biochemistry 36*, 13688−13692.
23. Venkatesan, P., and Kaback, H. R. (1998) *Proc. Natl. Acad. Sci. U.S.A. 95*, 9802−9807.
24. Zhao, M., Zen, K.-C., Hubbell, W., and Kaback, H. R. (1999) *Biochemistry 38*, 7407−7412.
25. Sahin-Tóth, M., le Coutre, J., Kharabi, D., le Maire, G., Lee, J. C., and Kaback, H. R. (1999) *Biochemistry 38*, 813−819.
26. Wolin, C. D., and Kaback, H. R. (2000) *Biochemistry 39*, 6130−6135.
27. Carrasco, N., Antes, L. M., Poonian, M. S., and Kaback, H. R. (1986) *Biochemistry 25*, 4486−4488.
28. Carrasco, N., Puttner, I. B., Antes, L. M., Lee, J. A., Larigan, J. D., Lolkema, J. S., Roepe, P. D., and Kaback, H. R. (1989) *Biochemistry 28*, 2533−2539.
29. Weinglass, A. B., and Kaback, H. R. (1999) *Proc. Natl. Acad. Sci. U.S.A. 96*, 11178−11182.
30. Teather, R. M., Bramhall, J., Riede, I., Wright, J. K., Furst, M., Aichele, G., Wilhelm, V., and Overath, P. (1980) *Eur. J. Biochem. 108*, 223−231.
31. Ho, S. N., Hunt, H. D., Horton, R. M., Pullen, J. K., and Pease, L. R. (1989) *Gene 77*, 51−59.
32. Consler, T. G., Persson, B. L., Jung, H., Zen, K. H., Jung, K., Prive, G. G., Verner, G. E., and Kaback, H. R. (1993) *Proc. Natl. Acad. Sci. U.S.A. 90*, 6934−6938.
33. Sanger, F., Nicklen, S., and Coulsen, A. R. (1977) *Proc. Natl. Acad. Sci. U.S.A. 74*, 5463−5467.
34. Kaback, H. R. (1971) *Methods Enzymol. 22*, 99−120.
35. Short, S. A., Kaback, H. R., and Kohn, L. D. (1975) *J. Biol. Chem. 250*, 4291−4296.
36. Kaback, H. R. (1974) *Methods Enzymol. 31*, 698−709.
37. West, I. C. (1970) *Biochem. Biophys. Res. Commun. 41*, 655−661.
38. Sahin-Tóth, M., and Kaback, H. R. (1993) *Protein Sci. 2*, 1024−1033.
39. Peterson, G. L. (1977) *Anal. Biochem. 83*, 346−356.
40. Newman, M. J., Foster, D. L., Wilson, T. H., and Kaback, H. R. (1981) *J. Biol. Chem. 256*, 11804−11808.
41. Franco, P. J., and Brooker, R. J. (1994) *J. Biol. Chem. 269*, 7379−7386.
42. Sahin-Tóth, M., Dunten, R. L., Gonzalez, A., and Kaback, H. R. (1992) *Proc. Natl. Acad. Sci. U.S.A. 89*, 10547−10551.
43. Lee, J. L., Hwang, P. P., Hansen, C., and Wilson, T. H. (1992) *J. Biol. Chem. 267*, 20758−20764.
44. Sahin-Tóth, M., and Kaback, H. R. (1993) *Biochemistry 32*, 10027−10035.
45. Lolkema, J. S., Puttner, I. B., and Kaback, H. R. (1988) *Biochemistry 27*, 8307−8310.
46. Sahin-Tóth, M., Akhoon, K. M., Runner, J., and Kaback, H. R. (2000) *Biochemistry 39*, 5097−5103.
47. Garcia, M. L., Viitanen, P., Foster, D. L., and Kaback, H. R. (1983) *Biochemistry 22*, 2524−2531.
48. Frillingos, S., and Kaback, H. R. (1996) *Biochemistry 35*, 10166−10171.

BI002171M